

FATIGUE LIFE PREDICTION OF ADDITIVE MANUFACTURED MATERIALS USING A DEFECT SENSITIVE MODEL

Muztahid Muhammad, Patricio E. Carrion, Nima Shamsaei*

National Center for Additive Manufacturing Excellence (NCAME),
Department of Mechanical Engineering, Auburn University, Auburn, AL.

*Corresponding author:
Email: shamsaei@auburn.edu
Phone: (334) 844 4839

Abstract

This study utilized a defect sensitive fatigue model based on a fracture mechanics concept to predict the fatigue life of 17-4 precipitation hardening (PH) stainless steel (SS) fabricated using laser beam powder bed fusion (LB-PBF) process. Size of defects such as gas entrapped pores are captured using fractography analysis and calculated employing Murakami's approach with the \sqrt{area} method. Considering the value of the \sqrt{area} as initial crack length, fatigue life is then calculated using NASGRO software, and compared to the experimental data obtained from strain-controlled fatigue testing. A comparison between predicted fatigue lives using NASGRO software, combined with the Murakami approach, and experimentally obtained ones were presented to determine the applicability of the utilized model for predicting the fatigue performance of additive manufactured materials.

Keywords: Additive manufacturing, defect size, NASGRO, fatigue life prediction.

Introduction

Additive manufacturing (AM), a layer-wise manufacturing method, enables fabricating parts with complex geometries layer by layer [1–3]. The development in AM technologies has revamped a broad spectrum of industries by introducing the potential of manufacturing parts with complex structure, functionally graded materials, and even assemblies, which are often challenging for conventional fabricating processes [4]. Among different AM methods, laser beam powder bed fusion (LB-PBF) is one of the most commonly used. This method uses a laser beam to fabricate parts from a pre-deposited layer of powder [5]. Similar to other AM methods, LB-PBF offers numerous benefits like cost reduction, smaller equipment footprint, reduced labor cost, reduced manufacturing time, no mold and pattern, and most significantly, it could offer enhanced mechanical properties [6]. However, along with numerous advantages, the unique thermal processing history experienced during AM induces many challenges like tensile residual stresses, and the formation of defects like pores, and lack of fusion [1, 6]. Poor surface finish as a result from the repetitious scanning during printing specimens also facilitates crack nucleation. These process-inherent defects are very detrimental when the part is subjected to cyclic loading, as it may lead to premature fatigue failure [2, 7]. In order to address these issues about the structural integrity

of AM parts under cyclic loading conditions, it is crucial to develop a model which can successfully predict fatigue life behavior of additively manufactured materials.

17-4 precipitation hardening (PH) stainless steel (SS), being a suitable candidate material for AM, can be widely used to manufacture complex parts with minimum wastage. 17-4 PH SS possesses excellent mechanical properties like high strength, fracture toughness, and corrosion resistance at both ambient and service temperature (below 300°C) after appropriate heat treatment. Due to the above-mentioned properties, 17-4 PH SS is extensively used in various applications including aviation, power plants, petrochemical, and marine applications [8]. However, when used in the fabrication of additively manufactured parts, inherent residual stresses have proven detrimental to fatigue and mechanical properties [9]; hence, post-process heat treatments have been employed to improve the overall mechanical performance of AM 17-4 PH SS. Therefore, it is critical to address the specific type of heat treatment condition, its effects on the fatigue behavior of 17-4 PH SS, and incorporate them when attempting to use fatigue life prediction model [10].

Until now, numerous researchers followed different approaches to model fatigue life behavior of additive manufactured materials [12, 13]. Torries et al., to calculate the fatigue life of AM Ti-6Al-4V, employed microstructure sensitive fatigue (MSF) model [14–16]. Beretta et al. [17], and Romano et al. [18, 19] adopted ‘defect tolerant design’ concept based on ‘Kitagawa-Takahashi’ diagram to model fatigue behavior of additive manufactured materials. NASGRO is a well-known fatigue behavior analysis tool based on fracture mechanics approach [20]. Murakami’s \sqrt{area} method [21, 22] is one of the promising approaches to measure the crack size based on the projection of the defect size on the loading plane in the loading direction, which can be incorporated in NASGRO crack growth equation to calculate fatigue life. However, to the best of authors knowledge, based on Murakami’s approach, using the NASGRO crack propagation equation to assess the fatigue life performance of the LB-PBF 17-4 PH SS after CA-H900 heat treatment has not been studied hitherto.

Here, this study aimed to develop a defect sensitive fatigue model to predict the fatigue life of LB-PBF 17-4 PH SS using fracture mechanics approach based on the known defect population of the material. As an effort to predict the fatigue life, NASGRO software was used to calculate fatigue life using the inherent defect size of the materials based on Murakami’s approach, and a comparison between NASGRO predicted fatigue lives and experimentally obtained values were presented to determine the applicability of this model for predicting the fatigue performance of AM materials.

Material and Specimen Fabrication

Using argon-atomized 17-4 PH SS powder, the samples were prepared in EOS M290 additive manufacturing machine using standard process parameter. Square bar and net-shape round specimens were fabricated and fatigue tests were conducted after employing CA-H900 heat treatment [23] on the LB-PBF 17-4 PH SS specimens. Square bars (11 mm X 11mm X 77 mm) were machined to the uniform round specimen and both the as-built and machined specimens have the similar final dimensions of 15 mm uniform gauge length with 5 mm gauge diameter. For CA-H900 heat treatment, samples were heated at 1050°C for 30 minutes followed by air-cooling. Then, the samples were heated at 482°C for 1 hour. Detailed results are reported in [23]. The experimental

fatigue life data used in this investigation was obtained by conducting strain-controlled uniaxial fully reversed ($R_\varepsilon = -1$) fatigue test in MTS landmark servohydraulic testing machine based on ASTM E606 standard [24] at ambient temperature. Fatigue crack growth data for LB-PBF 17-4 PH SS were adapted from [25]. To analyze defect sizes for LB-PBF 17-4 PH SS, a Keyence VHX-6000 microscope was used.

Defect Sensitive Fatigue Model

In general, there are three stages of fatigue life in a defect sensitive material: crack nucleation, crack propagation, and final fracture. When the material undergoes cyclic loading below the yield stress, crack nucleation occurs. The nucleation of the crack is typically attributed to the slip mechanisms. With the continuation of the loading cycles, the crack advances with the plastic deformation at the crack tip. When the crack size reaches the final fracture zone, i.e., critical crack size, final fracture occurs [26, 27]. However, with the current additive manufacturing technology, it is impossible to fabricate a defect-free part due to the formation of pores [1, 28]. These defects can act as a source for initial crack nucleation. These defects can be considered as pre-existing cracks playing the role of internal stress raiser. Therefore, the fatigue life of AM materials, in general, is mainly spent in the second stage, i.e., the crack propagation phase [15, 19, 29–31]. Therefore, to appropriately evaluate the fatigue life of AM parts, it is critical to consider AM inherent defects as pre-existing cracks during the crack propagation phase. Currently, there are three approaches for calculating fatigue life considering these structural features: fracture mechanics, the multistage fatigue model (MSF), and numerical modeling [7].

Stress intensity factor, K , indicates the state of unstable or rapid crack propagation without any increment of applied stress. Based on fracture mechanics, the maximum stress intensity factor experienced in the material by the defects can be calculated as [22]:

$$K_{max} = Y\sigma_{max}\sqrt{\pi a_i} \quad (1)$$

K_{max} is the maximum stress intensity factor, σ_{max} is the maximum applied stress, Y is the shape factor, and a_i is the initial defect size.

As previously mentioned, calculation of the critical defect size is necessary for accurate fatigue life predictions of AM materials. Murakami's \sqrt{area} approach is a well-established method for the estimation of effective size of irregular defects and interacting adjacent defects for fatigue design [32], and has proved reliable when used in fatigue life calculations [21, 22]. In this approach, a threshold stress at the tip of cracks developing from inherent defects, e.g. pores or LoFs, is determined to calculate fatigue life of the specimen by employing equation (1). The initial defect size was estimated by measuring the square root of the defect area projected in the direction of applied loading and then the value was input into the equation. This approach is location sensitive, and therefore, for surface cracks, stress intensity factor is stated as:

$$K_{max} = 0.65\sigma_{max}\sqrt{\pi\sqrt{area}} \quad (2)$$

For internal defect, stress intensity factor:

$$K_{max} = 0.5\sigma_{max}\sqrt{\pi\sqrt{area}} \quad (3)$$

In conventional fracture mechanics approach, the relationship between the stress intensity factor range and crack growth rate determines the fatigue crack growth behavior. Crack is nucleated in the crack nucleation zone, and this zone is mainly controlled by factors like microstructure, mean stress, etc. Crack propagation zone depends on the relationship between the crack size corresponding to the number of cycles to the stress intensity factor [33].

$$\frac{da}{dN} = C(\Delta K)^n \quad (4)$$

Here, a is the crack length, N is the number of cycles, C is a intercept constant, and n is the slope of crack growth rate and stress intensity plotting on a log-log scale.

After obtaining the value of stress intensity factor, K , it is feasible to get the fatigue crack growth life by integrating the sigmoidal curve of fatigue behavior between the limits of initial defect size and final defect size. However, employing equation (4) is not enough to accurately calculate the correct fatigue behavior of materials as it is not capable to accounts for stress ratio. NASGRO crack growth equation is one of the most general crack growth equation used to calculate the fatigue life of a material, and is given by equation (5) [20]:

$$\frac{da}{dN} = C \left[\left(\frac{1-f}{1-R} \right) \Delta K \right]^n \frac{\left(1 - \frac{\Delta K_{th}}{\Delta K} \right)^p}{\left(1 - \frac{K_{max}}{K_c} \right)^q} \quad (5)$$

Here, C is the intercept constant for $R=0$, f is the Newman crack closure function, R is the fatigue stress ratio, ΔK is the stress intensity range, n is the slope on a log-log scale, ΔK_{th} is the threshold stress intensity range, K_c is the critical stress intensity, K_{max} is the maximum stress intensity in the range of ΔK and p and q are the empirical coefficients determining crack growth rate in the initial and final stage of fatigue, i.e., in the crack nucleation and final fracture zone respectively. NASGRO software also considered the effect of crack closure while calculating the fatigue life. In this research, only the life of the fatigue crack propagation stage was calculated, and the values of p and q were assumed as 0. Therefore, the equation used in this study is:

$$\frac{da}{dN} = C \left[\left(\frac{1-f}{1-R} \right) \Delta K \right]^n \quad (6)$$

Results and Discussion

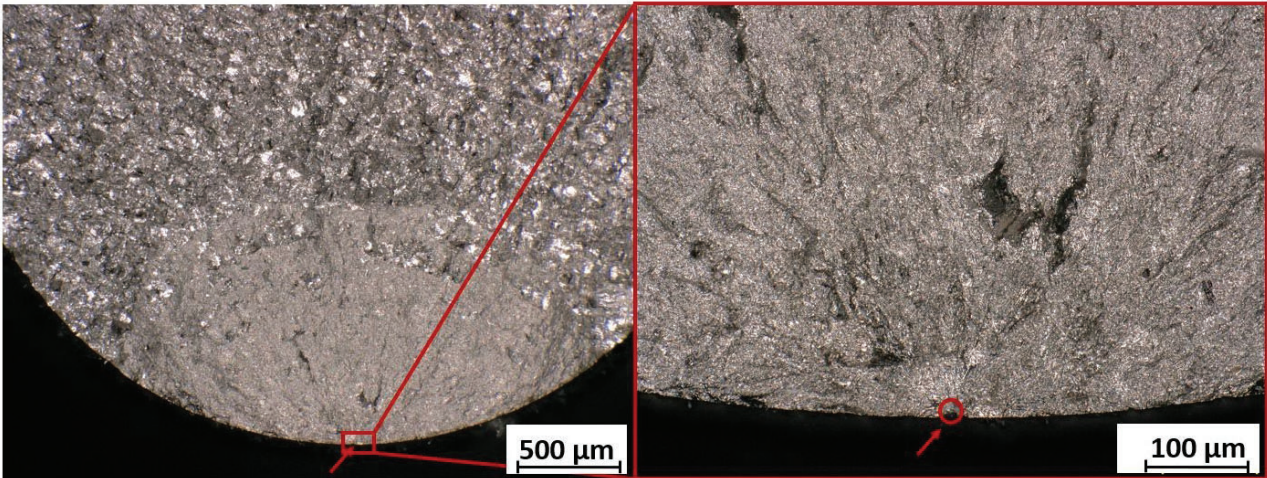


Figure 1: Crack initiation from defects (pore) for machined LB-PBF 17-4 PH SS after CA-H900 heat treatment

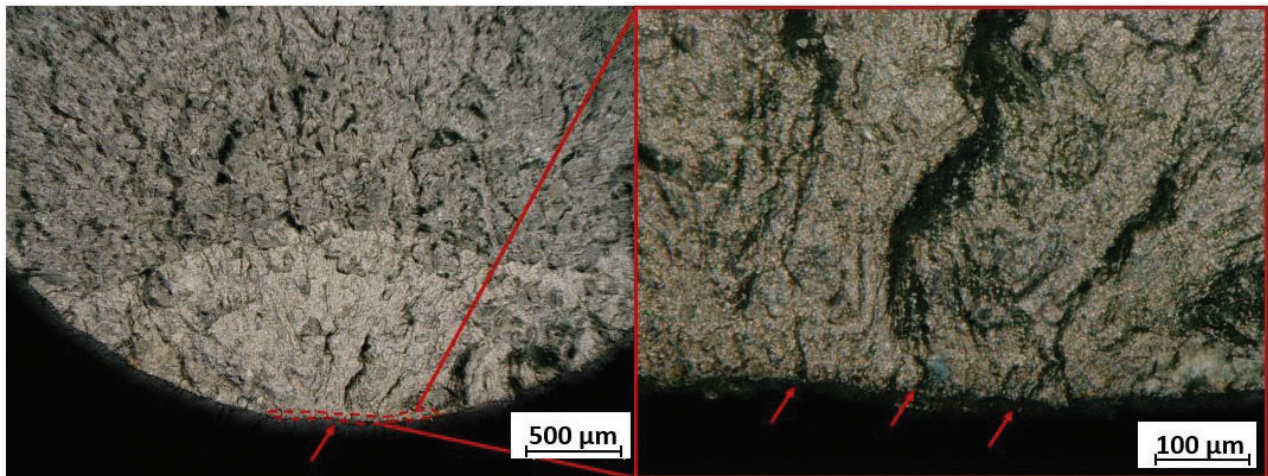


Figure 2: Crack initiation from the micro-notches of the boundary surface for as-built LB-PBF 17-4 PH SS after CA-H900 heat treatment

Figure 1 and 2 demonstrate the crack initiation site of machined and as-built LB-PBF 17-4 PH SS, respectively. The crack nucleation sites are marked with red arrows and, for machined specimens, the crack sources are marked with red circle. For machined specimens, the source of crack initiation is uniform round pores. According to the Murakami's approach, size of the pores was analyzed to calculate the defect size [21]. On the other hand, as-built specimens have multiple micro-notches on the surface due to poor surface finish attributed to the additive manufacturing process, which might act as a source of crack initiation. These micro-notches make it challenging to measure defect size accurately. Hence, for AM parts, considering the post-contour process, a scanning strategy after melting the powder at the edge of the surface for better surface finish, a conservative approach may be followed to determine the crack size of as-built parts [34]:

$$\sqrt{\text{area}_{\text{as-built}}} \cong d\sqrt{10} \quad (7)$$

Here, d is the width of the area covering the post-contour process on the circular fracture surface of the specimen, which is typically within the range of 60-80 μm for LB-PBF process employing EOS machine.

Figure 3 demonstrates the fatigue life correlations between the NASGRO predictions and experimental fatigue life of LB-PBF 17-4 PH SS in both as-built and machined conditions after CA-H900 heat treatment. In Figure 3, blue line demonstrates the perfect fit line and orange dashed lines demonstrate the scatter band of factor of 2. Scatter bands of a factor of 2 are also included for data comparison. Fatigue life was calculated according to the equation (6) and (7), utilizing fracture mechanics approach. Although CA-H900 procedure of LB-PBF 17-4 PH SS demonstrates superior mechanical properties (such as high strength), its fatigue performance is poor. Due to the high strength obtained after CA-H900 procedure, the material is highly sensitive to defects such as LoF, which decreases the fatigue resistance of the material specifically in high cycle fatigue regime [35]. From Figure 3, it is observed that 100% of the predicted fatigue data are within the scatter band of factor of 2 for both as-built and machined LB-PBF 17-4 PH SS specimens. For machined specimens, mostly a non-conservative prediction is observed for both low cycle fatigue and high cycle fatigue regime. For as-built specimens, mostly conservative predictions were observed.

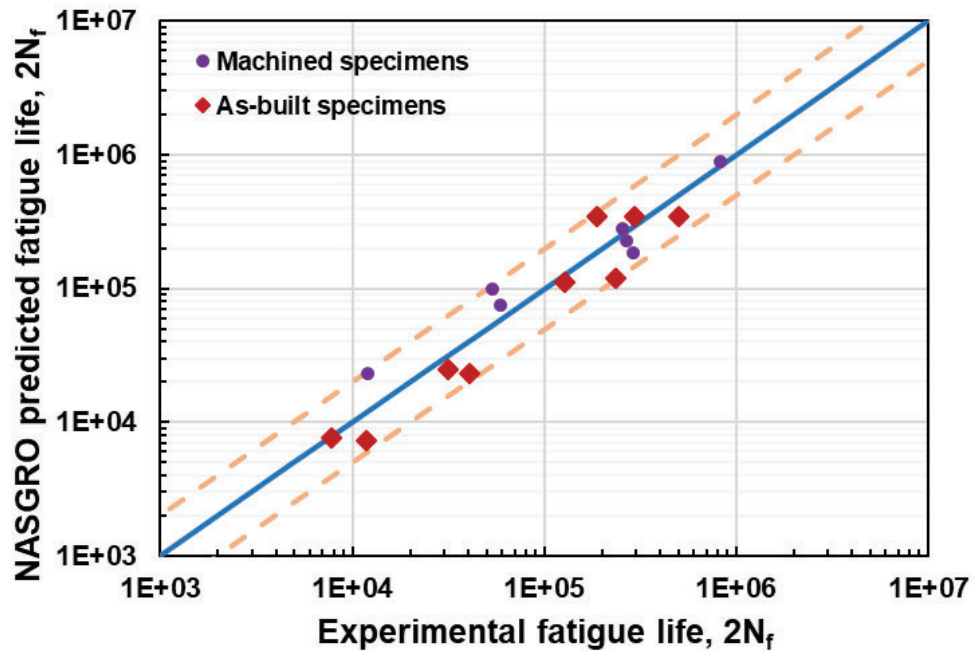


Figure 2: NASGRO calculated fatigue life correlation to the experimental fatigue life of both as-built and machined LB-PBF 17-4 PH SS after CA-H900 heat treatment

Conclusions

In this study, the fatigue life prediction of LB-PBF 17-4 PH SS was investigated based on fracture mechanics approach employing Murakami's \sqrt{area} method. This investigation can be summarized as follows:

- NASGRO crack growth equation incorporating Murakami's \sqrt{area} approach is capable to predict the fatigue life behavior of both as-built and machined LB-PBF 17-4PH SS for CA-H900 heat treatment conditions.
- Fatigue life predictions obtained using NASGRO, for both as-built and machined LB-PBF 17-4 PH SS specimens, fall within scatter bands of factor of 2, which shows that the estimated fatigue life is in good agreement with the experimental fatigue life.
- A non-conservative fatigue life prediction is obtained for machined LB-PBF 17-4 PH SS for CA-H900 heat treatment conditions which might be attributed to the better surface finish of machined samples.
- A conservative fatigue life prediction is obtained for as-built LB-PBF 17-4 PH SS for CA-H900 heat treatment conditions which is accounted to the conservative approach employed due to poor surface finish.

Acknowledgment

The authors greatly acknowledge for the support provided by the National Science Foundation under grant #1657195.

References

- [1] N. Shamsaei, A. Yadollahi, L. Bian, and S. M. Thompson, "An overview of Direct Laser Deposition for additive manufacturing; Part II: Mechanical behavior, process parameter optimization and control," *Addit. Manuf.*, 2015.
- [2] S. R. Daniewicz and N. Shamsaei, "An introduction to the fatigue and fracture behavior of additive manufactured parts," *International Journal of Fatigue*, 2017.
- [3] T. DebRoy *et al.*, "Additive manufacturing of metallic components – Process, structure and properties," *Progress in Materials Science*. 2018.
- [4] K. V. Wong and A. Hernandez, "A Review of Additive Manufacturing," *ISRN Mech. Eng.*, 2012.
- [5] S. Bremen, W. Meiners, and A. Diatlov, "Selective Laser Melting. A manufacturing technology for the future?," *Laser Tech. J.*, vol. 9, pp. 33–38, 2012.
- [6] A. Yadollahi and N. Shamsaei, "Additive manufacturing of fatigue resistant materials: Challenges and opportunities," *Int. J. Fatigue*, 2017.
- [7] B. Torries, A. Imandoust, S. Beretta, S. Shao, and N. Shamsaei, "Overview on Microstructure- and Defect-Sensitive Fatigue Modeling of Additively Manufactured Materials," *JOM*. 2018.
- [8] P. Tsipouridis, "Mechanical properties of Dual-Phase steels," *PhD Thesis*, 2006.
- [9] A. Yadollahi, N. Shamsaei, S. M. Thompson, A. Elwany, and L. Bian, "Effects of building orientation and heat treatment on fatigue behavior of selective laser melted 17-4 PH stainless steel," *Int. J. Fatigue*, 2017.
- [10] A. Bayode, S. Pityana, E. T. Akinlabi, and M. B. Shongwe, "Effect of scanning speed on

- laser deposited 17-4PH stainless steel,” in *Proceedings of 2017 8th International Conference on Mechanical and Intelligent Manufacturing Technologies, ICMIMT 2017*, 2017.
- [11] Y. Sun, R. J. Hebert, and M. Aindow, “Effect of heat treatments on microstructural evolution of additively manufactured and wrought 17-4PH stainless steel,” *Mater. Des.*, 2018.
- [12] Y. Xue, A. Pascu, M. F. Horstemeyer, L. Wang, and P. T. Wang, “Microporosity effects on cyclic plasticity and fatigue of LENSTM-processed steel,” *Acta Mater.*, 2010.
- [13] Y. Xue, H. El Kadiri, M. F. Horstemeyer, J. B. Jordon, and H. Weiland, “Micromechanisms of multistage fatigue crack growth in a high-strength aluminum alloy,” *Acta Mater.*, 2007.
- [14] B. Torries and N. Shamsaei, “Fatigue Behavior and Modeling of Additively Manufactured Ti-6Al-4V Including Interlayer Time Interval Effects,” *JOM*, 2017.
- [15] B. Torries, A. J. Sterling, N. Shamsaei, S. M. Thompson, and S. R. Daniewicz, “Utilization of a microstructure sensitive fatigue model for additively manufactured Ti-6Al-4V,” in *Rapid Prototyping Journal*, 2016.
- [16] B. Torries, R. Shrestha, A. Imandoust, and N. Shamsaei, “Fatigue Life Prediction of Additively Manufactured Metallic Materials Using a Fracture Mechanics Approach,” pp. 1181–1190, 2018.
- [17] S. Beretta and S. Romano, “A comparison of fatigue strength sensitivity to defects for materials manufactured by AM or traditional processes,” *Int. J. Fatigue*, 2017.
- [18] S. Romano, L. Patriarca, S. Foletti, and S. Beretta, “LCF behaviour and a comprehensive life prediction model for AlSi10Mg obtained by SLM,” *Int. J. Fatigue*, 2018.
- [19] S. Romano, A. Brandão, J. Gumpinger, M. Gschweidl, and S. Beretta, “Qualification of AM parts: Extreme value statistics applied to tomographic measurements,” *Mater. Des.*, 2017.
- [20] R. G. Forman, V. Shivakumar, J. W. Cardinal, L. C. Williams, and P. C. McKeighan, “Fatigue crack growth database for damage tolerance analysis,” 2005.
- [21] Y. Murakami and M. Endo, “Effects of defects, inclusions and inhomogeneities on fatigue strength,” *Int. J. Fatigue*, 1994.
- [22] M. Yukiitaka and E. Masahiro, “Quantitative evaluation of fatigue strength of metals containing various small defects or cracks,” *Eng. Fract. Mech.*, 1983.
- [23] P. D. Nezhadfar, R. Shrestha, N. Phan, and N. Shamsaei, “Fatigue behavior of additively manufactured 17-4 PH stainless steel: Synergistic effects of surface roughness and heat treatment,” *Int. J. Fatigue*, 2019.
- [24] ASTM E606/E606M, “Standard Test Method for Strain-Controlled Fatigue Testing,” *ASTM Standards*. 2012.
- [25] P. D. Nezhadfar *et al.*, “Fatigue crack growth behavior of additively manufactured 17-4 PH stainless steel: Effects of build orientation and microstructure,” *Int. J. Fatigue*, 2019.
- [26] A. Fatemi *et al.*, “Fatigue behaviour of additive manufactured materials: An overview of some recent experimental studies on Ti-6Al-4V considering various processing and loading direction effects,” *Fatigue and Fracture of Engineering Materials and Structures*. 2019.
- [27] R. R. I. Stephens, A. Fatemi, R. R. I. Stephens, and H. O. Fuchs, *Metal Fatigue in Engineering*. 2000.
- [28] H. Gong, K. Rafi, H. Gu, T. Starr, and B. Stucker, “Analysis of defect generation in Ti-6Al-4V parts made using powder bed fusion additive manufacturing processes,” *Addit. Manuf.*, 2014.

- [29] A. J. Sterling, B. Torries, N. Shamsaei, S. M. Thompson, and D. W. Seely, "Fatigue behavior and failure mechanisms of direct laser deposited Ti-6Al-4V," *Mater. Sci. Eng. A*, 2016.
- [30] N. Shamsaei and J. Simsiriwong, "Fatigue behaviour of additively-manufactured metallic parts," *Procedia Struct. Integr.*, 2017.
- [31] A. S. Johnson, S. Shao, N. Shamsaei, S. M. Thompson, and L. Bian, "Microstructure, Fatigue Behavior, and Failure Mechanisms of Direct Laser-Deposited Inconel 718," *JOM*, 2017.
- [32] H. Masuo *et al.*, "Influence of defects, surface roughness and HIP on the fatigue strength of Ti-6Al-4V manufactured by additive manufacturing," *Int. J. Fatigue*, 2018.
- [33] P. C. Paris, M. P. Gomez, and W. E. Anderson, "A rational analytic theory of fatigue," *Trend Eng.*, 1961.
- [34] Y. Murakami, *Effects of Small Defects and Nonmetallic Inclusions on the Fatigue Strength of Metals*. 2009.
- [35] A. Yadollahi, N. Shamsaei, S. M. Thompson, A. Elwany, and L. Bian, "Effects of building orientation and heat treatment on fatigue behavior of selective laser melted 17-4 PH stainless steel," *Int. J. Fatigue*, 2017.